*Journal of Structural Geology*, Vol. 7, No. 5, pp. 605 to 612, 1985
Printed in Great Britain

0191–8141/85 $03.00 + 0.00


# Extension and rifting: the Zeit region, Gulf of Suez

J. ANGELIER

Tectonique Quantitative, Département de Géotectonique, Université P. et M. Curie,
4 place Jussieu, 75230 Paris Cedex 05, France

(*Received* 8 *May* 1984; *accepted in revised form* 1 *November* 1984)

**Abstract**—A field analysis of faults and fractures in the Ras Gharib–Ras Gemsa region of the Gulf of Suez shows that the main Late Cenozoic extension occurred perpendicular to the rift axis. Three main types of dip-slip normal faults successively developed as the tilt of blocks bounded by antithetic normal faults increased. Determinations of the amount of extension from structural data are compatible with estimates made using subsidence data through a simplified model of lithospheric stretching. The uplift of rift shoulders is related in chronology and volume to the subsidence of the rift. The geometry of fault patterns and directions of extension suggests that the Late Cenozoic total movement corresponds to a counterclockwise rotation of 4–5° of Sinai relative to Africa, with a pole close to Cairo.

## INTRODUCTION

THE GULF of Suez is the northwesternmost portion of the Late Cenozoic Red Sea rift system. North of 27°30′N, the continuity of the rift is interrupted by a NNE–SSW trending zone of left-lateral shear and locally extension, the Gulf of Aqaba–Dead Sea Rift transform fault system (Eyal *et al.* 1981). Together with the Mediterranean margin and the folded Syrian arc (Eyal & Reches 1983), the rift of the Gulf of Suez and the strike-slip graben of the Gulf of Aqaba define a triangular Sinai 'microplate' (Robson 1971). The geology of the Gulf of Suez region has been described in numerous papers (e.g. Garfunkel & Bartov 1977) and information has been provided during petroleum research (e.g. Gilboa & Cohen 1979, Abdine 1981). A study of the Ras Gharib–Ras Gemsa region illustrates the mechanisms of Late Cenozoic normal faulting and rift opening (Figs 1 and 2).

## STRUCTURE AND LATE CENOZOIC HISTORY

Most of our knowledge of the geology of the area south of Ras Gharib is derived from recent studies (Burollet *et al.* 1982). The main structural trends are NW–SE, that is, parallel to the axis of the Gulf of Suez. South of Dara, two major basement blocks (Zeit and Melaha) are tilted to the southwest and bounded by large normal faults to the northeast. Between these main blocks, the Zeit basin is a deep graben with a 3.5–5.0 km thick Late Cenozoic infill (Abdine 1981, El Heiny & Martini 1981); crests of smaller blocks are present. North of Dara, the pattern of tilted blocks (as the Gharamul hills) is less regular; Miocene faulted monoclines, plateaus and gentle folds dominate. The Dara ridge itself is a WSW–ENE transverse zone with evidence of early tectonic activity (Burollet *et al.* 1982). Large differences between the Late Cenozoic structural patterns dominated by NW–SE trends north and south of the Dara ridge indicate that transform strike-slip movements took place along this transverse zone during rift extension.

The crests of the main uplifted blocks, as well as the Gharib massif to the west, belong to the metamorphic and igneous Precambrian–Palaeozoic basement cut by numerous NE–SW and NW–SE dykes. This basement is

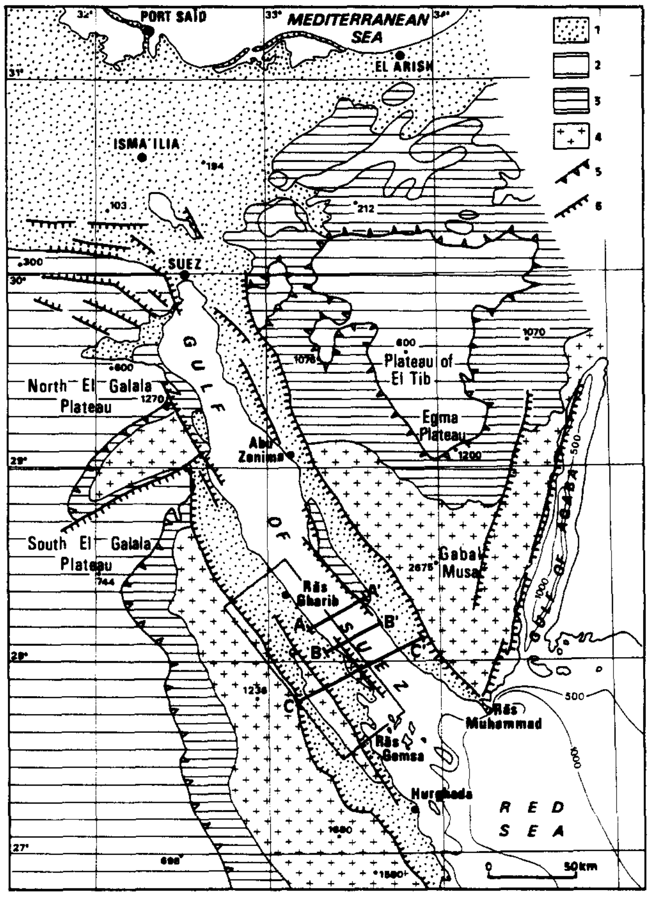


Fig. 1. Geological map of the Gulf of Suez. 1, Oligocene to Quaternary; 2, Eocene; 3, Nubian to Late Cretaceous; 4, pre-Nubian basement; 5, scarp bordering Eocene plateaus; 6, main faults. Quadrangle: location of studied area. AA′, BB′ and CC′, locations of cross-sections shown in Fig. 4.

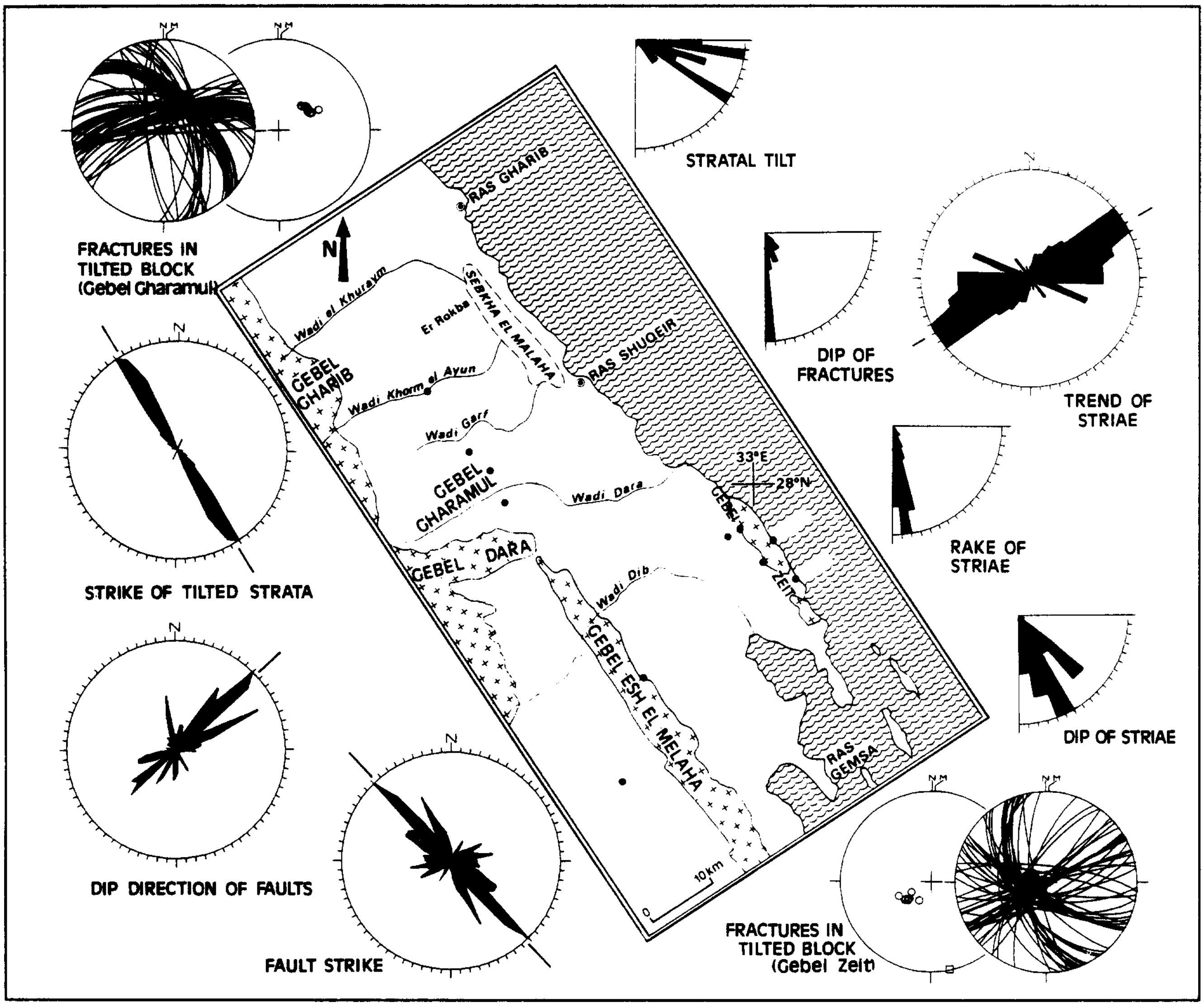


Fig. 2. Fault-fracture geometry. Strike, dip and rake (pitch) distributions for 403 faults and fractures, 61 slickenside lineations and 88 bedding attitudes. Pairs of diagrams: Schmidt's projections (lower hemisphere) of fracture planes (thin curves) and poles to bedding (open circles).

unconformably overlain by the Nubian sandstones, and Late Cretaceous and Eocene sequences. No relation exists between the Cretaceous–Eocene palaeogeography and the Late Cenozoic one in the region of the Gulf of Suez, indicating that no 'proto-gulf' of Suez had developed prior to the Oligocene (Garfunkel & Bartov 1977).

Radiometric dating of a basic intrusion in the transverse Dara zone has yielded a late Oligocene age (Burollet *et al.* 1982). This intrusion probably belongs to the Early Cenozoic, mainly Oligocene, igneous phase commonly related to the initial faulting of the Suez rift (e.g. Garfunkel & Bartov 1977). Although little is known about the initial phase of rifting, drill-hole and seismic reflection data in the Gulf oil fields show that in most cases the oldest Miocene sediments overlie the top of the pre-Miocene formations, provided that the stratigraphic section has not been altered by further erosion (Gilboa & Cohen 1979, Abdine 1981). These observations show that no important doming occurred prior to rifting (because the more recent pre-rift terranes, the Eocene limestones, are often present in the axial zone of the Gulf, whereas doming should have induced erosion), and also that no widespread block tilting took place prior to the Early Miocene (because the oldest Miocene formation is in most cases approximately concordant on the Eocene).

The Late Cenozoic sediments include three main groups (pre-evaporitic, evaporitic and post-evaporitic) which roughly correspond to the Early Miocene, to the Middle–Late Miocene and to the Plio-Quaternary, respectively (e.g. Garfunkel & Bartov 1977). The pre-evaporitic sediments are mainly sandy and sometimes conglomeratic; marls and shales are abundant and numerous limestone bodies belong to reefal and peri-reefal formations; variations in facies are rapid and frequent. The Early Miocene palaeogeography was dominated by complex patterns of small troughs, reefs, islands and channels controlled by uplift and subsidence of faulted-tilted blocks. Schematic sections of the main oil fields of the Gulf of Suez (Robson 1971, Gilboa & Cohen 1979, Abdine 1981) indicate that in many cases the structure of faulted-tilted blocks already existed at the end of the pre-evaporitic phase; numerous oil fields correspond to crests of tilted blocks buried beneath thick evaporites. During the Early Miocene, many block crests were eroded and often capped or surrounded by reefs, while thick clastics were deposited on their flanks and in adjacent troughs. Fault movements and limited tilting continued during the evaporitic and post-evaporitic periods.

## FAULT AND FRACTURE GEOMETRY IN OUTCROPS

About six hundred measurements of Late Cenozoic tectonic features were collected in the Ras Gharib–Ras Gemsa area (Fig. 2). Among 403 faults and fractures, only 61 faults bear slickenside lineations. 110 tension gashes and 88 attitudes of bedding were also measured. The discontinuity of outcrops separated by Quaternary sediments, alluvium and dunes probably introduces some bias into the sampling of measurements in terms of azimuthal frequencies. The localization of many sites along block crests and cliffs that trend parallel to the Gulf favours measurements of transverse and oblique fractures. In contrast, the importance of the transverse Dara zone is underestimated in diagrams because the largest portion of this structure is hidden beneath recent deposits.

As the diagrams of stratal strikes and dips show, the tilted blocks generally trend N145–150°E, parallel to the axis of the Gulf; their dips range from 5 to 35°, in most cases to the SW. Steeper dips were observed (40–55° in the pre-Miocene strata of Gebel Zeit). Most faults also strike N135–140°E. This distribution defines a typical extensional pattern of tilted blocks bounded by antithetic faults. Smaller sets of fault strikes are present, for example, N080°E, N120–125°E and N155°E. The dips of faults with noticeable stratigraphic offsets range from 40 to 80° and average 60–70°. Fractures and joints dip approximately vertical in horizontal or gently tilted blocks, but may have gentler dips in significantly tilted blocks. 50% of slickenside lineations have pitches greater than 70°: fault mechanisms are normal, commonly dip-slip. This distribution explains why most trends of striae range from N50°E to N65°E, perpendicular to the main fault strikes and to the axis of the Gulf (Fig. 2). For about two thirds of the fault sets, lateral slip (always very small relative to normal dip-slip) is dextral. However, as only 61 striated fault surfaces were observed, it is impossible to determine whether this distribution of minor lateral slip is significant or not.

As illustrated in two pairs of diagrams, joints and fractures are generally approximately perpendicular to bedding planes (Fig. 2); they developed during the early stages of extension and block faulting, and have subsequently undergone rotation due to block tilting. This geometry does not depend on the sense (and amount) of stratal tilt. In many sites, such fractures commonly strike either approximately parallel to the NW–SE tilt axis (their deviation from the vertical equals the dip of strata) or approximately perpendicular to the tilt axis (they remain vertical regardless of block tilting). Fractures parallel to the Gulf are probably nascent tension gashes, because actual tension gashes with the same attitude are present.

In the Gebel Zeit where the stratal dips are the steepest, reactivation of NW–SE trending fractures perpendicular to bedding is inferred from the presence of numerous parallel and closely-spaced normal faults and joints: faults show dip-slip offsets of strata, but cannot be distinguished otherwise from adjacent joints.

An analysis of aerial photographs shows that the strikes of the main fault systems average N150–155°E (Gharib and Dara) and N135–160° (Melaha and Zeit), whereas other large faults trend NNE–SSW, NNW–SSE, ENE–WSW and NE–SW. Large longitudinal (N135–145°E) and transverse (N50–60°E) fractures affect the Miocene. The fracture trends detected on aerial photographs are thus in agreement with local measurements, which consequently can be considered representative (Fig. 2).

## PALAEOSTRESS ORIENTATION

The methods for determining the reduced tensor giving the axes of maximum compressive stress ($\sigma_1$), intermediate stress ($\sigma_2$) and minimum stress ($\sigma_3$), as well as the ratio $\Phi = (\sigma_2-\sigma_3)/(\sigma_1-\sigma_3)$ (Angelier 1984) have been applied to fault slip data in three areas (Fig. 3). Consistent determinations show that the $\sigma_1$ axis is vertical while the average $\sigma_3$ axis trends N55°E, that is, perpendicular to the Gulf axis. Fault geometry already indicated that extension approximately trends N50–65°E, parallel to the main direction of dip-slip striae of normal faults (Fig. 2). The distribution of vertical tension gashes independently suggests that $\sigma_3$ was horizontal and trended approximately N45°E (Fig. 3).

Block tilting does not affect palaeostress reconstructions for three reasons: it is limited in most sites, most fault slip data correspond to the last stages of faulting, and the moderate tilts of dip-slip normal faults that strike parallel to tilt axis barely affect tensor determinations.

In detail, the variation of $\sigma_3$ directions in the transverse Dara zone (Fig. 3) may correspond to a dextral strike-slip component of extensional motion. Determinations are not numerous enough to confirm this hypothesis. In the Zeit and Melaha ranges, as well as in the Araba range on the opposite shore of the Gulf, the fault-tilt axes strike N145–150°E in the basement and N140–145°E in the Miocene. This constant difference may correspond to a small counterclockwise variation in the direction of extension during the Miocene. The simplicity of the main fault systems, however, suggests that no major change occurred in the area during the widespread Late Cenozoic extension.

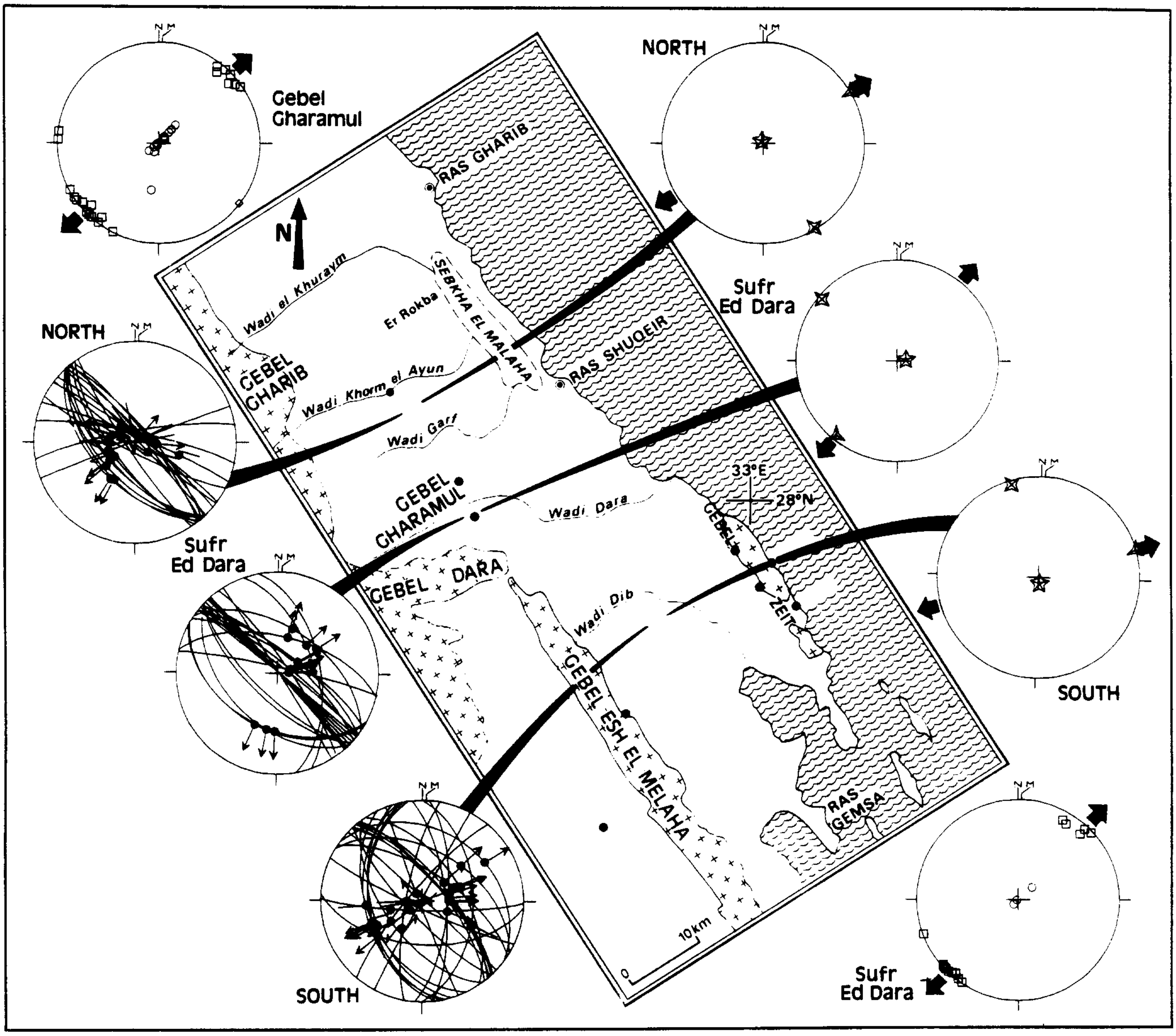


Fig. 3. Determinations of palaeostress axes from Late Cenozoic faults. Diagrams are Schmidt's projections of lower hemisphere. On left, fault slip data used (dots with small arrows designate slickenside lineations). On right, corresponding principal axes of computed palaeostress tensors; $\sigma_1$, $\sigma_2$ and $\sigma_3$ axes as 5, 4 and 3-branch stars, respectively. Two diagrams illustrate populations of tension gashes (poles as squares); open circles are poles to bedding. Large black arrows: directions of extension.

## EVOLUTION OF BLOCK TILTING AND FAULTING

Field analyses of major and minor structures locally provide accurate determination of attitudes of fault-fracture systems, but large portions of tilted blocks are hidden. Geological sections reconstructed using seismic-reflection profiles and borehole data (e.g. Meshref & Hammouda 1982, Abdine 1981) show that the structural pattern is dominated by large tilted blocks, typically 10–30 km wide, bounded by normal faults and often divided into smaller blocks (Fig. 4). The amount of tilt varies from less than 10° (Melaha) to about 20° (July and Ramadan oil fields) or even 40° (Gebel Zeit). The faults that originally separated the blocks have often been tilted and cut by younger and steeper faults; after correction, one commonly obtains an initial average fault dip of 55–70° in Miocene or Eocene terranes. Geological mapping on the opposite shore of the Gulf revealed similar dips (Chenet & Letouzey 1983). These values of 55–70° are within the usual range of dips typical of dip-slip normal faults. Similarly, numerous conjugate systems of minor normal faults, which are symmetrically distributed relative to tilted bedding planes and consequently developed prior to most of the tilting, had initial fault dips of 55–70°.

Another source of dispersion of the dips of large normal faults is the variable original depth, depending on the amount of later erosion in outcrops. A major fault dips only 50°E west of Dara. Because the present outcrop was about 1 km deep before erosion and uplift, the dip probably decreased with depth (taking into account steeper fault dips where erosion has remained small).

The large antithetic dip-slip normal faults that first

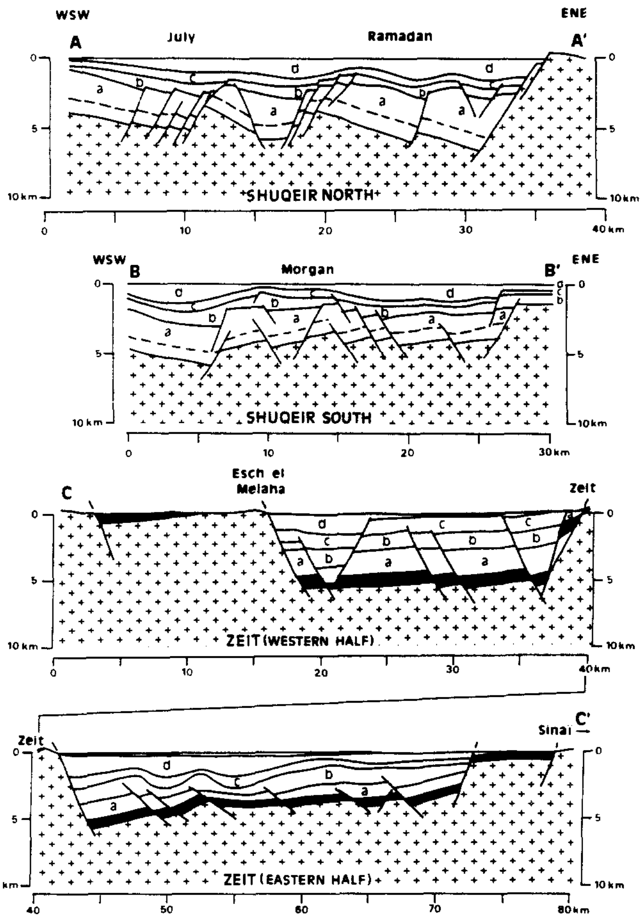


Fig. 4. Sections across the Gulf of Suez between Ras Gharib and Ras Gemsa. Modified after Meshref & Hammouda 1982 (Shuqeir oil field sections) and Abdine 1981 (Zeit section). Pattern of crosses: basement. Black: pre-Miocene sediments (Nubian–Cretaceous–Eocene) of Zeit section (approximate top shown as dashed line in Shuqeir sections). a, Miocene (pre-evaporitic series); b, Miocene evaporites; c, Miocene (post-evaporitic series); d, Plio-Quaternary. Locations of sections AA', BB' and CC' in Fig. 1.

separated the major blocks are 'first-order normal faults'. Smaller faults belong to the same conjugate system. Minor tension fractures that were originally vertical are abundant. All these structures ($F_1$, f and t in Fig. 5a) strike approximately parallel to the NW–SE axis of subsequent tilting, which suggests that no major change in the direction of extension has occurred. Transverse and oblique structures include joints, minor fractures and larger fault zones comparable to those of Dara. Transverse joints may represent tension fractures perpendicular to secondary extension, while oblique fractures and large structures could well correspond to minor strike-slip and to transform motion within the framework of rift extension, respectively.

Where the amount of tilt has become greater than approximately 30°, many joints have begun to act as normal faults. These 'second-order normal faults', perpendicular to bedding ($F_2$ in Fig. 5b and c), divide the major first-order blocks into smaller second-order blocks as tilt increases. Such faults have not been observed in moderately tilted blocks, although joints are present. In the last stage of faulting, a new generation of steeply-dipping first-order normal faults developed ($F_3$ in Fig. 5d) and they define horsts and grabens, such as the present Zeit range and basin. Although accurate observation is difficult on the downthrown side of major fault scarps, these faults probably cut and offset the original pattern of tilted blocks. This reconstruction, which needs confirmation, resembles that discussed by Morton & Black (1975). The relation between the first- and second-order normal faults can be easily interpreted in terms of internal deformation of major blocks required by increasing tilt (Angelier & Colletta 1983). The relation between the first- and the second-generation of large normal faults, $F_1$ and $F_3$, is less clear and the development of $F_3$ faults is not obviously related to tilt increase. In addition, the distinction $F_2$–$F_3$ is difficult. The transition between the first- and the second-generation of major faults probably occurred during the Early Miocene. The first generation ($F_1$ and $F_2$) was active during the first period of extension and intense block tilting that characterize the Zeit and Melaha blocks, the second generation ($F_3$) controlled the further subsidence of the Zeit basin and the uplift of the adjacent block crests (partly explained by moderate continuing tilt). This change could correspond to the major rearrangement of fault patterns that occurred 16–15 Ma ago in the Gulf of Suez, according to Garfunkel & Bartov (1977).

## AMOUNT OF EXTENSION

Using overall cross-sections within the Gulf (e.g. Abdine 1981, Meshref & Hammouda 1982) supported by local accurate field measurements of stratal tilt and fault dips, and adopting Mesozoic and Early Cenozoic reference levels, a simple analysis of cross-sections in terms of reconstructed stratal lengths shows that the average factors of extension ($\beta$) (final surface divided by initial surface) range from 1.2 to 1.3 in the Shuqeir and Zeit segments of the rift (Fig. 4). However, because most faults with stratigraphic offsets smaller than about 100 m are neglected in such geological sections, the actual amount of extension should be significantly larger (minor faults are so numerous that the resulting deformation is not negligible). Continuous deformation of sediments, which is limited, has also been neglected. Local estimates of $\beta$ based on accurate field data close to block crests have provided values of 1.1 to about 2, but cannot be extrapolated. Finally, the average regional factor of extension determined in the transverse section of the Gulf (Chenet & Letouzey 1983) and that given here using comparable data (Fig. 4) are similar (1.2–1.4).

The method adopted for estimating the stretching factor, $\beta$, using subsidence data is based on the simplest models of lithospheric stretching (McKenzie 1978, Le Pichon & Sibuet 1981). In detail, the reasoning is the same as that presented elsewhere for the Sea of Crete (Angelier *et al.* 1982), but the age of 25 Ma for the extension implies that thermal subsidence reached about 15–18% of the thermal subsidence after infinite time. As several important factors are neglected (e.g.

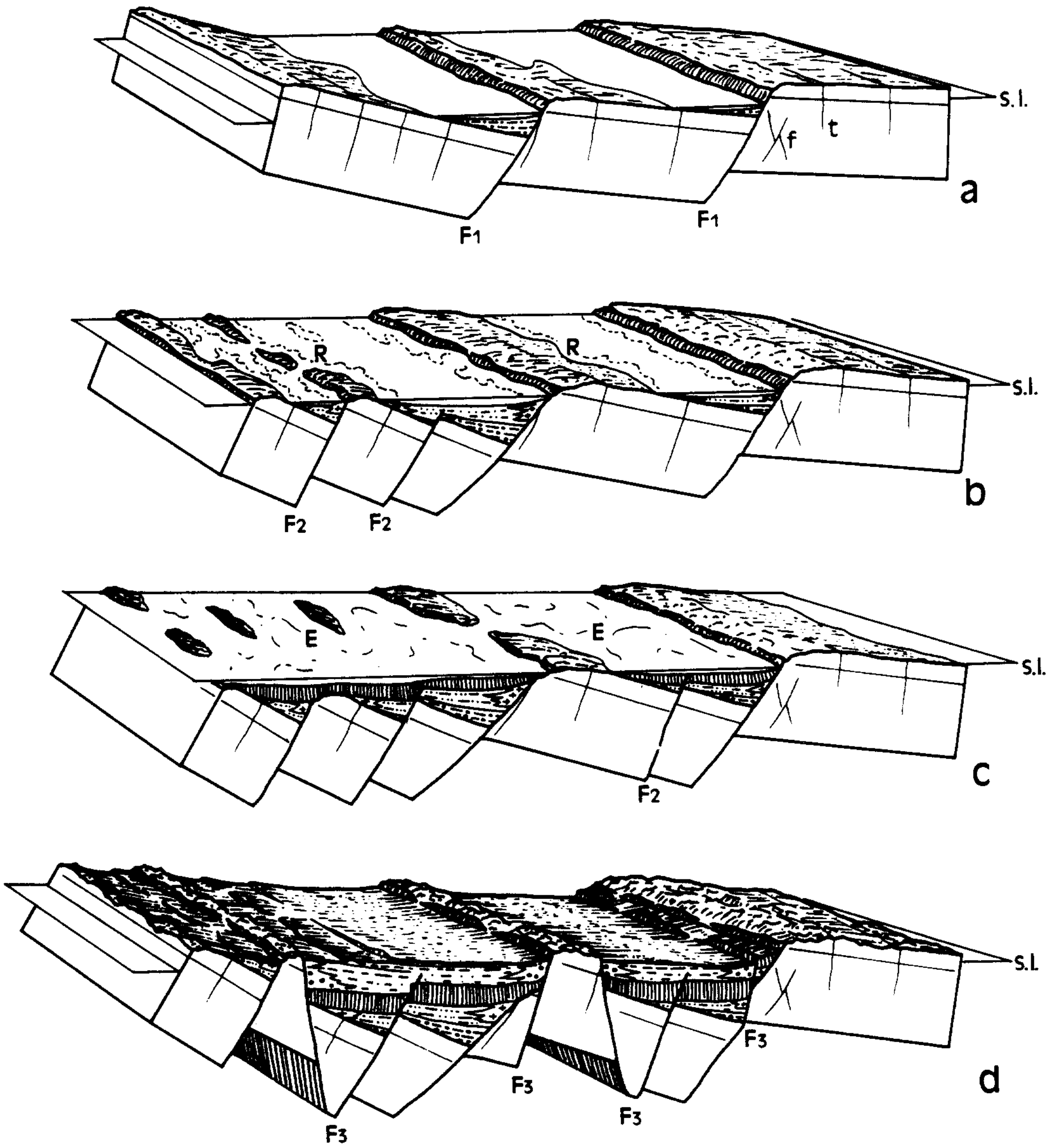


Fig. 5. Evolution of a system of tilted blocks (schematic). s.l., sea-level; a, Late Oligocene–Early Miocene (F1, first-order normal faults, first generation; f, conjugate normal fault systems; t, tension fractures); b, Early Miocene (F2, second-order normal faults, first generation; R, reefs); c, Middle Miocene (E, evaporitic basins; evaporites vertically ruled in section); d, Present (F3, first-order normal faults, second generation).

heterogeneous stretching, lateral cooling and thermal effect of sedimentation), one can only obtain a rough estimate of the magnitude of extension. In the absence of water and sediments, the present virtual subsidence $Z^*$ is

$$Z^* = \left(1 - \frac{1}{\beta}\right)(2.96 + a), \quad (1)$$

where $a$ is the initial elevation in km. After adding water (depth $b$, in km) and sediments (thickness $s$ in km, with a density of 2.4 g cm$^{-3}$), one obtains

$$\beta = \frac{4.35 + 1.47a}{4.35 - b - 0.37s}. \quad (2)$$

Compilation of available data (Abdine 1981, El Heiny & Martini 1981, Meshref & Hammouda 1982, Hagras & Slocki 1982) indicates that $s$ averages 3.6–3.7 km for the Late Cenozoic of the Shuqeir–Zeit sections of the Gulf (Fig. 4); $b$ is smaller than some tens of metres; a value of 0.4 km has been adopted for $a$ (as in the Eastern Desert of Egypt). These parameters lead to determine an average stretching factor, $\beta$, of 1.65–1.7 in the central zone of the rift, now 55 km wide (i.e. 33 km before rifting). Using data from two drill-holes, Chenet & Letouzey (1983) obtained similar values ($\beta = 1.7$). For the entire rift section, now 80 km wide, one obtains an average value of 1.45–1.5 (i.e. a width of 55 km before rifting).

These estimates of extension using subsidence data are significantly larger than the estimates independently obtained by geometrical analysis of cross-sections. The difference is probably accounted for by the underestimation made while neglecting minor structures and internal deformation in geometrical analysis, and possibly also by the large simplifications implicit in the estimate of extension from subsidence data. Finally, an extension with an average $\beta$ coefficient of 1.4–1.5 for the whole rift (now 80 km wide) and of 1.6–1.7 for the axial basins (now 55 km wide) corresponds to an amount of total opening of about 25 km along the Zeit section of the rift. These estimates imply that the factor of extension, $\beta$, related to small-scale faulting (offsets smaller than 100 m) and continuous deformation within the axial zone averages 1.2–1.3.

## RIFT SUBSIDENCE AND SHOULDER UPLIFT

Isopach maps (e.g. Hagras & Slocki 1982) show that the average volume of pre-evaporitic sediments per km of Gulf decreases from north (56 $km^3$ $km^{-1}$) to south (38 $km^3$ $km^{-1}$). The sediments of the southern Gulf contain a large proportion of sand that originated in the basement and the Nubian Sandstone, so that the computed total volume of sand in the Lower Miocene sediments increases from 1.5 $km^3$ $km^{-1}$ to 10.5 $km^3$ $km^{-1}$ from north to south. This variation corresponds to the uplift of rift shoulders south of 29°N (Fig. 1), resulting in a large influx of clastic sediments in the adjacent grabens.

The amount of uplift of the massifs on both sides of the Gulf reaches 3–5 km, taking into account the erosion of Nubian and Cretaceous–Eocene sediments. Overall sections suggest that the eroded volume per km of Gulf in the Zeit region averages 80 $km^3$ for the western shoulders and 100 $km^3$ for the eastern ones. The total volume of Late Cenozoic clastics in the rift sediments per km of Gulf averages 150 $km^3$, that is about 125 $km^3$ of basement rock. Thick sediment infills are present close to uplifted and eroded basement rocks, as in the Zeit basin adjacent to the Melaha block. It is likely that the present drainage pattern continued that of the Miocene (Gilboa & Cohen 1979). The rough correspondence between the volume of clastics in the Gulf sediments and the eroded volume of the rift shoulders is consistent with the synchronism between rift subsidence and shoulder uplift. Other studies have revealed domal uplift of Sinai beginning about 26–27 Ma ago and continuing during most of the Miocene with at least 3 km of uplift post-dating 9 Ma ago (Kohn & Eyal 1981). These observations suggest that the shoulder uplift is driven by isostatic adjustment related to the thermal effects that accompany rift extension and subsidence.

## DISCUSSION AND CONCLUSIONS

The Late Cenozoic extensional pattern of the Ras Gharib–Ras Gemsa area of the Gulf of Suez corresponds, in first approximation, to the pure transverse opening of a rift with predominantly dip-slip normal faults. Strike-slip faults and palaeostress changes are certainly present but play a minor role. This is ascertained by the simplicity and consistency of fault-fracture data sets collected in the area (Figs. 2 and 3). This simplicity, in turn, explains why consistent results can be obtained using small data sets. In contrast, large data sets are required in order to decipher palaeostress distribution and evolution in areas where tectonic history has been complicated and polyphase, as in Aegea (e.g. Angelier *et al.* 1982): in such complex areas, small data sets display large heterogeneity and cannot be used for reliable palaeostress reconstructions at the regional scale.

The Late Cenozoic extensional deformation of the area is dominated by the development of series of tilted fault blocks (Fig. 4), with progressive activation or reactivation of several fracture sets as tilt increases (Fig. 5). Widespread block tilting occurred during the pre-evaporitic period (Early Miocene). First-order normal faults ($F_1$) separated the main blocks. Second-order normal faults ($F_2$) developed when normal slip occurred along pre-existing tension fractures perpendicular to bedding, thus dividing the main blocks into smaller blocks. This 'Zeit stage', however, is mainly limited to blocks that underwent amounts of tilting as large as 30° (Angelier & Colletta 1983). A new generation corresponds to steep normal faults ($F_3$), which probably contribute to the definition of major units such as the Zeit basin or the Zeit range. This sequence of two main generations of normal faults has already been identified in other rift areas (Morton & Black 1975).

In the area studied, the main successive fault families, $F_1$, $F_2$ and $F_3$, strike parallel to tilt axes within a range of 5–10°. Thus, they have probably developed within a single pattern of major extension and rift opening. Although several aspects of faulting and fracturing obviously require additional analyses to be made (for example, the role of pre-existing faults and the development of oblique to perpendicular fracture systems and strike-slip transform zones), there is no reason to suspect major palaeostress changes within the main phase of Late Cenozoic extension with the field observations analyzed here.

Along the western shore of the southern Gulf of Suez where N145°E trends dominate (Fig. 6), the direction of extension inferred from analyses of faults and palaeostress tensor reconstructions is N55°E (Figs. 2 and 3), that is identical to the eastern shore (Chenet & Letouzey 1983). To the north, the trends of the main systems of normal faults change to N125–130°E (northern Gulf), and then to approximately E–W (between Suez and Cairo). Provided that these major systems correspond to pure extension as in the south, this distribution of fault trends and inferred directions of extension suggests that the pole of opening of the Gulf (the pole or rotation of the Sinai region relative to Africa) is located close to Cairo, at the intersection of great circles perpendicular to the directions of extension (Fig. 6). Robson (1971) has already proposed a counterclockwise rotation of Sinai. This conclusion is supported by the widening and deepening of the Gulf from Suez to Ras Muhammad, and by the increasing amounts of subsidence and related shoulder uplift.

This interpretation implies that the dominant directions of extension average N35–40°E in the northernmost Gulf of Suez. Between Cairo and Suez, expected directions of extension may range from NE–

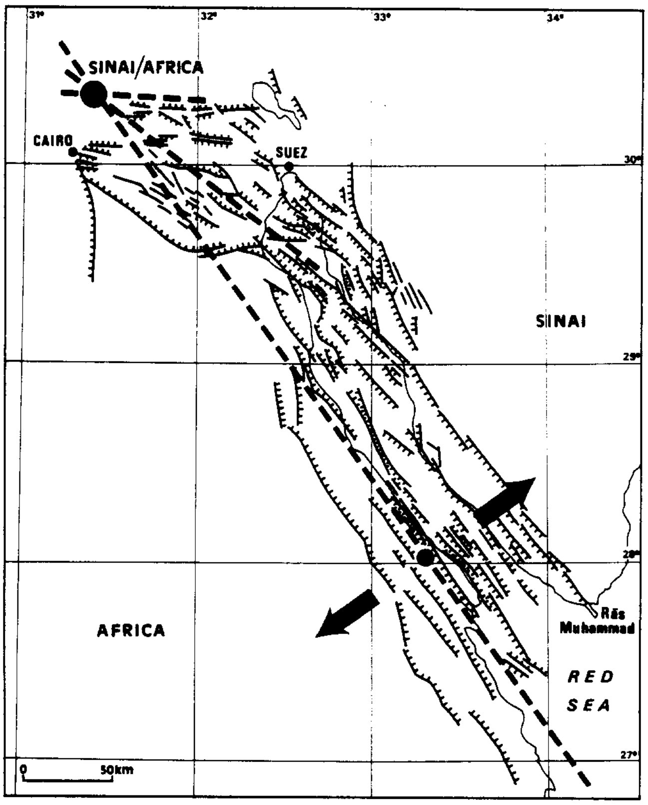


Fig. 6. Fault systems and kinematics of the Gulf of Suez. Main faults as barbed lines (barbs on the downthrown side). Large arrows, direction of extension in the studied area (black dot); thick dashed lines, axes of the main normal fault systems; largest black dot, proposed location of the Sinai/Africa pole of rotation.

SW to N–S, within a more complex fault pattern. This interpretation also implies that Late Cenozoic compression occurred in the Syrian Arc region, north of Sinai, provided that the southeastern tip of the Mediterranean Sea belongs to the African plate. Although the main NNW–SSE to N–S compression occurred during the Eocene, it is possible that this compressional regime continued into the Late Cenozoic (Eyal & Reches 1983).

Major structural differences exist between rift systems with extension at decreasing angles rift axes (Angelier & Bergerat 1983). Two contrasting cases are illustrated in the Sinai region: the Gulf of Suez where extension principally occurs transverse to the Gulf (Fig. 6), and the Gulf of Aqaba where left-lateral strike-slip prevails (Eyal *et al.* 1981). Strike-slip movements, however, are not absent in the Late Cenozoic evolution of the Gulf of Suez and correspond to zones of transform motion within the framework of extension (N–S to NNE–SSW sinistral zones between the southern and northern portions of the Gulf, and E–W to ENE–WSW dextral zone near Dara). Transverse and oblique Late Cenozoic fault systems partly correspond to older reactivated shear zones (Robson 1971, Garfunkel & Bartov 1977).

Adopting the estimate of 20–25 km for the total Sinai–Africa motion that occurred perpendicular to the Gulf in the Zeit region, one determines a total rotation of 4–5° counterclockwise of Sinai relative to Africa, since approximately 25 Ma ago.

*Acknowledgements*—Fieldwork was supported by the C.F.P. (Total Proche-Orient) and the I.F.P. (air fare). Mathematical analysis of data was supported by the A.T.P. of the C.N.R.S. Detailed field data are given in an unpublished report (1982). This study has been made possible by stratigraphic and structural information provided by P. F. Burollet, D. Templeton and M. Zaghloul (C.F.P.-Total). Geological maps of J. Boltze and Ph.Ott d'Estevou have been used. Discussions in the field with P. F. Burollet, G. Desforges, P. Gérard. X. Le Pichon and D. Templeton were fruitful.

## REFERENCES

Abdine, S. A. 1981. Egypt's petroleum geology: good grounds for optimism. *World Oil* December 1981, 99–112.

Angelier, J. 1984. Tectonic analysis of fault slip data sets. *J. geophys. Res.* **89**, 5835–5848.

Angelier, J. & Bergerat, F. 1983. Systèmes de contrainte et extension intra-continentale. Colloque "Rifts et Fossés anciens", Marseille. *Bull. Centre Rech. Explor.-Prod. ELF-Aquitaine* **7**, 137–147.

Angelier, J. & Colletta, B. 1983. Tension fractures and extensional tectonics. *Nature, Lond.* **301**, 49–51.

Angelier, J., Lyberis, N., Le Pichon, X., Barrier, E. & Huchon, P. 1982. The tectonic development of the Hellenic arc and the sea of Crete: a synthesis. *Tectonophysics* **86**, 159–196.

Burollet, P. F., Bolze, J. & Ott d'Estevou, Ph. 1982. Sedimentology and tectonics of the Gharamul area, West of Suez Gulf. *6th E.G.P.C. Exploration Seminar* Cairo, March 1982.

Chenet, P.-Y. & Letouzey, J. 1983. Tectonique de la zone comprise entre Abu Durba et Gebel Mezzazat (Sinai, Egypte) dans le contexte de l'évolution du rift de Suez. *Bull. Centre Rech. Explor.-Prod. ELF-Aquitaine* **7**, 201–215.

El-Heiny, I. & Martini, E. 1981. Miocene foraminiferal and calcareous nannoplankton assemblages from the Gulf of Suez region and correlations. *Géol. méditerr.* **8**, 101–108.

Eyal, M., Eyal, Y., Bartov, Y. & Steinitz, G. 1981. Tectonic development of the western margin of the Gulf of Elat (Aqaba) rift. *Tectonophysics* **80**, 39–66.

Eyal, Y. & Reches, Z. 1983. Tectonic analysis of the Dead Sea rift region since the Late Cretaceous based on mesostructures. *Tectonics* **2**, 167–185.

Garfunkel, Z. & Bartov, Y. 1977. The tectonics of Suez rift. *Bull. geol. Surv. Israel* **71**, 1–44.

Gilboa, Y. & Cohen, A. 1979. Oil trap patterns in the Gulf of Suez. *Israel J. Earth-Sci.* **28**, 13–26.

Hagras, M. & Slocki, S. 1982. Sand distribution of the Miocene clastics in the Gulf of Suez. *Proc. 6th E.G.P.C. Exploration Seminar* Cairo, March 1982.

Kohn, B. P. & Eyal, M. 1981. History of uplift of the crystalline basement of Sinai and its relation to opening of the Red Sea as revealed by fission track dating of apatites. *Earth Planet. Sci. Lett.* **52**, 129–141.

Le Pichon, X. & Sibuet, J.-C. 1981. Passive margins, a model of formation. *J. geophys. Res.* **86**, 3708–3720.

McKenzie, D. 1978. Some remarks on the development of sedimentary basins. *Earth Planet Sci. Lett.* **40**, 25–32.

Meshref, W. & Hammouda, H. 1982. Stripping techniques used in sea floor gravity. Interpretation of the South Belayim area, Gulf of Suez. *Proc. 6th E.G.P.C. Exploration Seminar* Cairo, March 1982.

Morton, W. H. & Black, R. 1975. Crustal attenuation in Afar. In *Afar Depression of Ethiopia* (edited by Pilger, A. & Rüsler, A.). Schweizerbart'sche Verlagsbuchhandlung, Stuttgart, 55–65.

Robson, D. A. 1971. The structure of the Gulf of Suez (Clysmic) rift, with special reference to the eastern side. *J. geol. Soc. Lond.* **127**, 247–276.